

RESEARCH PAPER

Enhanced Anti-corrosive Properties of Electrosynthesized Polyaniline/zeolite Nanocomposite Coatings on Steel

Mehdi Shabani-Nooshabadi *, Elaheh Allahyary and Yasser Jafari

Department of Analytical Chemistry, Faculty of Chemistry, University of Kashan, Kashan, Iran

ARTICLE INFO

Article History:

Received 14 February 2018

Accepted 10 March 2018

Published 01 April 2018

Keywords:

Coating

Corrosion

Electrosynthesis

Polyaniline/zeolite

nanocomposite

304 Stainless steel

ABSTRACT

The preparation of polyaniline/zeolite nanocomposite coating on 304 stainless steel (304 SS) surface has studied via the galvanostatic method. The electro-generated coating was characterized by Fourier transform infrared spectroscopy (FT-IR), UV-visible absorption spectroscopy, X-ray diffraction (XRD) patterns and scanning electron microscopy (SEM). The anticorrosion property of polyaniline/zeolite nanocomposite coating was explored in 0.5 M hydrochloric acid solution by Tafel polarization method and electrochemical impedance spectroscopy (EIS). The effect of variable parameters such as the applied current density and deposition time on the corrosion protection of the electro-generated coatings was also considered. The corrosion rate of coated-304 SS was released about 36 times lower than bare 304 SS. Potential of corrosion also changed from -0.411 V to -0.279 V versus Ag/AgCl for un-coated and coated-304 SS electrodes, respectively. Electrochemical measurements indicate that polyaniline/zeolite nanocomposite coated on 304 SS has remarkable inhibitive properties with protection effectiveness of ~97% at 2.5 mA cm⁻² current density used on 304 SS in acidic medium. The outcomes of this research obviously find out that the polyaniline/zeolite nanocomposite has an outstanding possible to defend 304 SS against corrosion in an acid environment.

How to cite this article

Shabani-Nooshabadi M, Allahyary E, Jafari Y. Enhanced Anti-corrosive Properties of Electrosynthesized Polyaniline/zeolite Nanocomposite Coatings on Steel. J Nanostruct, 2018; 8(2):131-143. DOI: 10.22052/JNS.2018.02.003

INTRODUCTION

Corrosion is the most devastating problem of modern technology and pose as a serious threat to many industries. Therefore, this is of paramount importance to scientists and engineers. Scientists not only peruse the corrosion behavior of metals/alloys in different environments, investigate the corrosion mechanism, but also finally aim to invention the operative methods to defend the materials. Corrosion plays a very main role in diverse fields of industry and, accordingly, in economics. Many documents and papers were issued each year about corrosion and corrosion protection of different metals. Among the metals studied, most investigation about corrosion

protection focuses on iron, since iron and its alloys are the basis of modern industry [1].

Iron and its alloys have broadly applied in many uses and diversity of these applications were intensified the researches relating to improvement of corrosion resistance of iron based metals in several neutral or aggressive environments [2-6]. Type 304 stainless steel (304 SS) appertains to a class of metals and alloys that have protected through an inactive film formed on their surface. Nevertheless, these alloys are vulnerable to localized attack; even high alloyed steels may destroy in strong chloride solutions. The localized corrosion of 304 SS is one of the most solemn problems facing the application of these

* Corresponding Author Email: m.shabani@kashanu.ac.ir

alloys [7]. This localized attack is a particularly important limitation of the material for biomedical applications [8]. The release of metal ions such as chromium, iron, and nickel in the biological environment surrounding the alloy results in a decreased biocompatibility. Numerous plans have been applied to produce more protective interfaces on stainless steels, containing the usage of conducting polymers [9].

Between the conducting polymers, polyaniline, and its derivatives have established the most attention due to their environmental and chemical constancy and their capability to switch reversibility from insulating state to conducting state were considered [10, 11]. Polyaniline has been more broadly considered as anti-corrosive coatings on many metals than its derivatives [12].

Polyaniline on metals are not perfect physical barriers contrary to corrosion when they are in connection with hostile species such as O_2 and H^+ . These corrosive species can reach the substrate via the coating defects [13]. Improving the current materials and developing new ones which are stronger, lighter, and more resistant to aggressive environments has concerned much attention. Conducting polymers are still of significant interest and importance as components for corrosion-resistant coatings [14, 15]. The polymeric materials can alter their molecular structure and consequently also their properties through reaction with a surrounding environment [16, 17].

The usage of polyaniline as corrosion protection coating of metals has been explored in many articles. Nevertheless, the porosity and the ion exchange capability of these polymeric coatings might be disadvantageous for corrosion protection performance. The charges loaded in the polymer layer can be irreversibly spent through the system's redox reactions, and the ability of the protection with polymer coatings may be missing with time. So, nanostructure materials such as nanocomposites have been produced due to their specific properties. To date, many documents have been published dealing with the chemical [18] and electrochemical [19, 20] methods and their corrosion protection properties were investigated. Electrochemically synthesis approaches are preferred because of the direct production of a polymer on the metal surface without any organic additives and ability of preparing smaller and size controllable particles by changing the used potential or the current density.

Inorganic/organic composites have been explored widely in recent years due to a wide range of potential use of these materials [21, 22]. One main class of such hybrid materials is that in which the organic portion has composed of conducting polymers, such as polyaniline or polypyrrole. It is hopeful to attain composite materials with synergetic or complementary manners between polymer and inorganic matrices. For example, polyaniline/inorganic composites with electrical and magnetic properties [23] have potential uses in batteries, electrochemical display devices, electromagnetic interference shielding, electromagnetorheological fluids [24], microwave-absorbing materials, and anticorrosion materials [25] due to their synergetic performances between conducting polymer and the inorganic magnetic nanoparticles.

Newly, inorganic solids with layered and porous structure have been used to confine and encapsulate into them conducting polymers to attain nanocomposite materials with fresh physicochemical properties [26, 27]. Particularly, the structure of zeolite, involving pores, channels, and cages of different shapes and dimensions of the nanometer order of magnitude, is predictable to protect the polymer from degradation, in which oxygen and wetness from the atmospheric air play a leading part. The isolation of the functional conducting polymer chains into the porous, and the improving of their alignment are predictable to decelerate aging and to increase their electrical conductivity. Moreover, the acidity of the zeolite surface ensures the outstanding adhesion of the two materials and a zeolite/conducting polymer system combines the fast electronic mobility of the polymer with the capability of the zeolite to accommodate transferable cations into its construction [28, 29].

As far as authors are aware, no earlier training on the preparation of polyaniline/zeolite nanocomposite onto 304 SS by galvanostatic procedure has been stated so far, and in this research, it is demonstrate for the first time that polyaniline/zeolite nanocomposite coatings can be electro-generated on 304 SS from the aqueous acidic electrolyte. The effect of variable parameters such as the applied current density and deposition time on the corrosion properties of the electro-generated coatings were also explored by polarization and EIS methods in 0.5 M hydrochloric acid solution. It also is presented

the characterization of the coatings by UV-vis absorption spectrometry, Fourier transform infrared spectroscopy (FTIR), X-ray diffraction (XRD) patterns and scanning electron microscopy (SEM).

MATERIALS AND METHODS

Zeolite Y was procured from Sigma-Aldrich. Other chemicals were procured from Merck. Aniline was newly distilled and kept in the dark. All solutions were newly provided from analytical grade chemical reagents consuming doubly distilled water. For every run, a newly ready solution and a cleaned set of electrodes were used, and all trials were carried out at room temperature. SAMA potentiostat/ galvanostat system (made in Iran) was applied for electrosynthesis and also, corrosion experiments were supported using a μ -AUTOLAB potentiostat/galvanostat model μ W AUTO71174 linked to a Pentium IV personal computer concluded a USB electrochemical interface. Prepared 304 SS was used as working electrode in the three-electrode cell. The metal piece was cut into rectangular samples of 1 cm² area, fused with Cu-wire for an electrical linking and mounted onto the epoxy resin to provide only one active flat surface exposed to the corrosive environment. Before every trial, the working electrode was polished with a sequence of emery papers of different marks (400, 800, 1000 and 1200), washed with doubly distilled water and degreased with acetone.

Electrosynthesis of polyaniline/zeolite nanocomposite coatings on 304 SS

Electrosynthesis was accomplished by galvanostatic test from an aqueous solution

having 20 mL of 0.5 M oxalic acid and 0.1 M aniline with 1 wt% of zeolite, a suitable quantity of zeolite was introduced into 100 mL of distilled water and was magnetically stirred for 3 hours at room temperature. Henceforth, a blend of 0.5 M oxalic acid and 0.1 M of aniline monomer was added into the zeolite solution under magnetic stirring for 1 h, afterward, the gained solution was ultrasonicated for 20 min to increase its uniformity. Production of polyaniline/zeolite nanocomposite coatings over the 304 SS surface was accomplished by applying a fixed current for certain duration of time. In this regard, densities of current of 0.5, 1, 2.5, and 5 mA cm² for the time duration of 100 s were applied, and the potential transients were recorded. Prepared 304 SS sample was used as the working electrode in the three-electrode assembly, with a Ag/AgCl (3 M KCl) electrode as the reference electrode and a graphite rod as the counter electrode. After the electrosynthesis stage, the green colored and homogeneous polyaniline/zeolite nanocomposite coatings (Fig. 1) were well attained on the 304 SS surface.

Characterization of electro-generated polyaniline/zeolite nanocomposite coatings

The electro-generated coating was dissolved in pure N-methylpyrrolidone (NMP), and UV-vis spectra of the polymer solution were recorded on a Perkin Elmer Lambda2S UV-vis spectrometer. The FTIR spectrum of the obtained coatings over the 304 SS surface was gotten with a Shimadzu Varian 4300 spectrophotometer in KBr pellets. The morphologies of the coated-304 SS surfaces were evaluated using a PHILIPS model XL30 scanning electron microscope instrument operating at 10 kV. XRD patterns were recorded by a Rigaku D-max

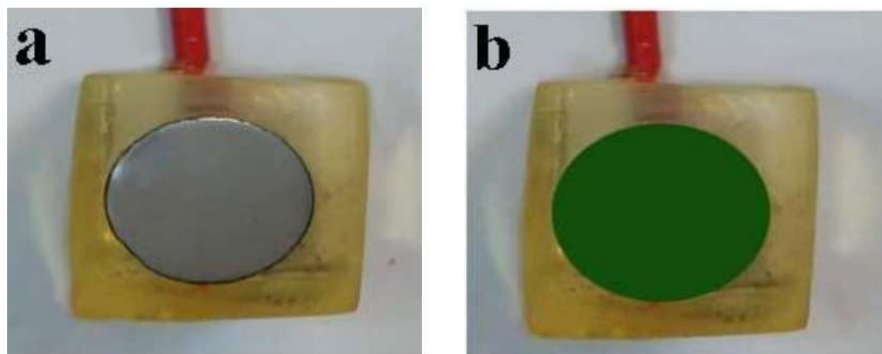


Fig. 1. The photographs of (a) un-coated and (b) polyaniline/zeolite nanocomposite-coated 304 SS electrodes.

C III X-ray diffractometer using Ni-filtered.

Corrosion experiments

The 304 SS samples covered with electro-generated polyaniline/zeolite nanocomposite coatings were assessed for their corrosion resistance properties in 0.5 M hydrochloric acid solution via Tafel polarization and electrochemical impedance spectroscopy (EIS). The coated 304 SS electrode was used as the working electrode in the three-electrode assembly, with an Ag/AgCl (3 M KCl) electrode as the reference electrode and a platinum sheet as the counter electrode. The working electrode was first dipped in the corrosive solution (0.5 M hydrochloric acid solution) for 60 min. In the case of Tafel polarization, the potential was scanned at ± 200 mV versus open circuit potential (OCP) at a scan rate of 0.5 mV s^{-1} . The Tafel regions were recognized from the anodic and cathodic polarization curves and extrapolated to the potential of corrosion (E_{corr}) for get the corrosion current density (i_{corr}) by the NOVA software. In the case of electrochemical impedance spectroscopy, a.c. signals of 20 mV amplitude and various frequencies from 100 kHz to 0.1 Hz at OCP were impressed to the coated-304 SS electrode. A Pentium IV-powered computer and

NOVA software were used for studying impedance data. All tests were done in a Faraday cage to minimize noise interferences.

RESULTS AND DISCUSSION

Electrochemical synthesis of the coatings on 304 SS

The experiments were done under galvanostatic conditions. The E-t transient curves were attained during the formation of polyaniline/zeolite nanocomposite coatings on 304 SS for four unlike applied current densities of 0.5, 1, 2.5 and 5 mA cm^{-2} (Fig. 2). As understood from the figure, the creation of polyaniline/zeolite nanocomposite coatings on 304 SS includes three separate stages: (I) adsorption of monomer and electrolyte and beginning of formation of passive film; (II) development and impingement of the passive film and breakdown of the latter; (III) creation of the nanocomposite coatings [30]. A homogeneous coating was attained at all applied current densities. The period to reach the maximum potential value is dissimilar for the applied current densities that it is designated as induction time.

As it can be realized in Fig. 2, the higher rates of formation can be achieved with the greater applied current densities, as predictable. Shorter induction

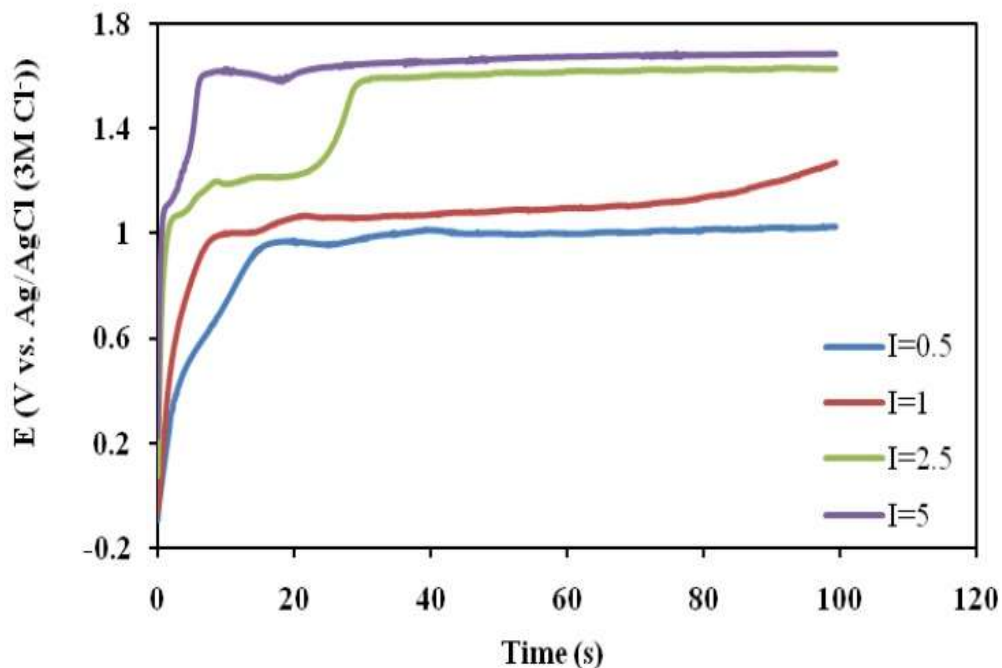


Fig. 2. E-t curves of the creation of the polyaniline/zeolite nanocomposite coatings on the 304 SS electrode in 0.5 M oxalic acid and 0.1 M aniline containing 1 wt% zeolite under galvanostatic conditions at various current densities.

times can be succeeded by applying upper current densities. The galvanostatic route provided the deposition of a green covering, characteristic of polyaniline/zeolite nanocomposite in the emeraldine oxidation state on the surface of 304 SS.

Characterization of the nanocomposite coatings

A typical FT-IR spectrum for polyaniline/zeolite nanocomposite having 1 wt% zeolite, polyaniline, and zeolite are shown in Fig. 3. The representative peaks were detected at 3432, 1628 and 1358 cm^{-1} , in contract with the works described [31-33]. The peak at 3432 cm^{-1} is due to the N- H stretching vibration of secondary amine. The peaks at 2924 and 2854 cm^{-1} are due to aromatic and aliphatic C-H stretching vibrations, respectively. The two peaks at 1358 and 1628 cm^{-1} are due to the benzenoid and quinoid groups, respectively. The peak at 1300 cm^{-1} is due to the aromatic N- H group. There are other representative peaks at 1210, 1130 and 570 cm^{-1} , due to 1,2,4-trisubstituted benzene rings. The Al-O stretching vibration at about 1024 cm^{-1} and O-T-O bending vibration at about 467 cm^{-1} authorize the existence of zeolite in the

nanocomposite coating [34, 35]. Obvious changes were observed for bands which are related to the structural OH vibrations in the region between 3500 cm^{-1} related to the bridging OH groups in, $\equiv\text{Al}-\text{OH}-\text{Si}\equiv$, and other hydrogen atom on different oxygen atoms in the frame work of zeolite. Hence, FTIR spectra of polyaniline/zeolite nanocomposite displays bands characteristic of polyaniline as well as of zeolite which approves the existence of both components in the coating.

UV-vis spectra of the polymer and nanocomposite samples were recorded at room temperature and are presented in Fig. 4. The UV-vis spectra of polyaniline/zeolite nanocomposite display an absorption band at 350 nm, and another broad weak peak around 600 nm. This first one matches to the π^* transition in the benzeneoid ring of the polymer [36]. The second at 600 nm can be ascribed to the exaction transition, which was rather weak in these polymers. The peak at 600 nm can be attributed to inter molecular transition among the benzeneoid and quinoid moieties in the polymer [37]. The UV-vis absorption spectra of the polyaniline/zeolite nanocomposite shown a blue shift from the peak location for pure

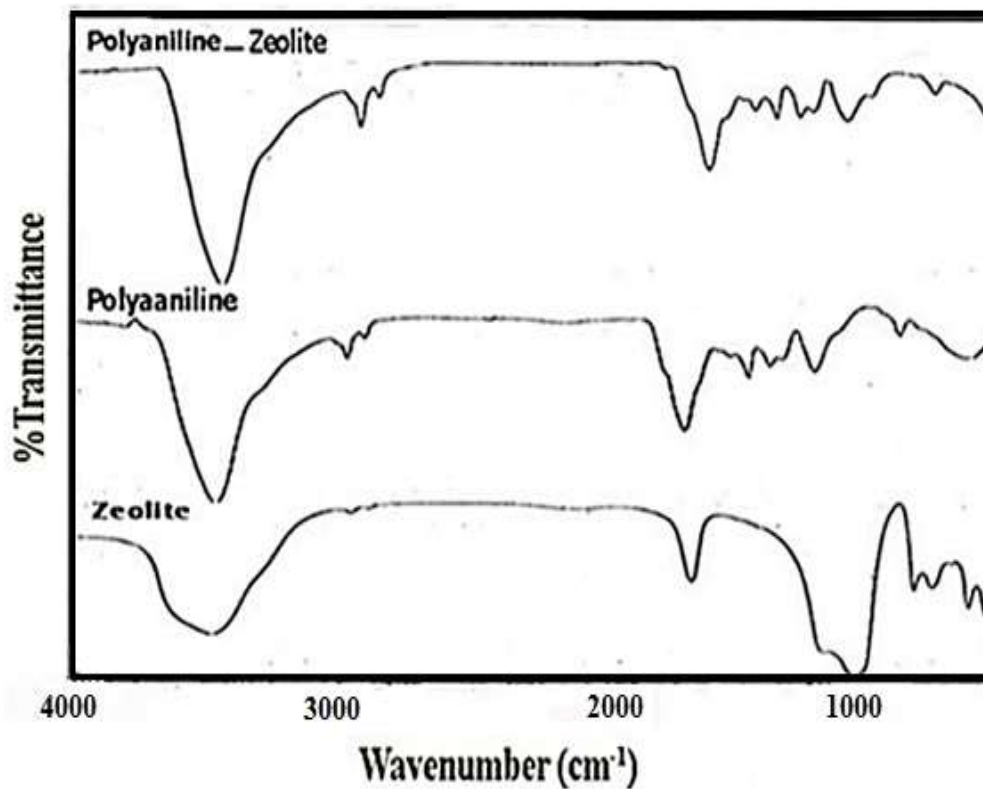


Fig. 3. FT-IR spectrum for zeolite, polyaniline and the polyaniline/zeolite nanocomposite coating.

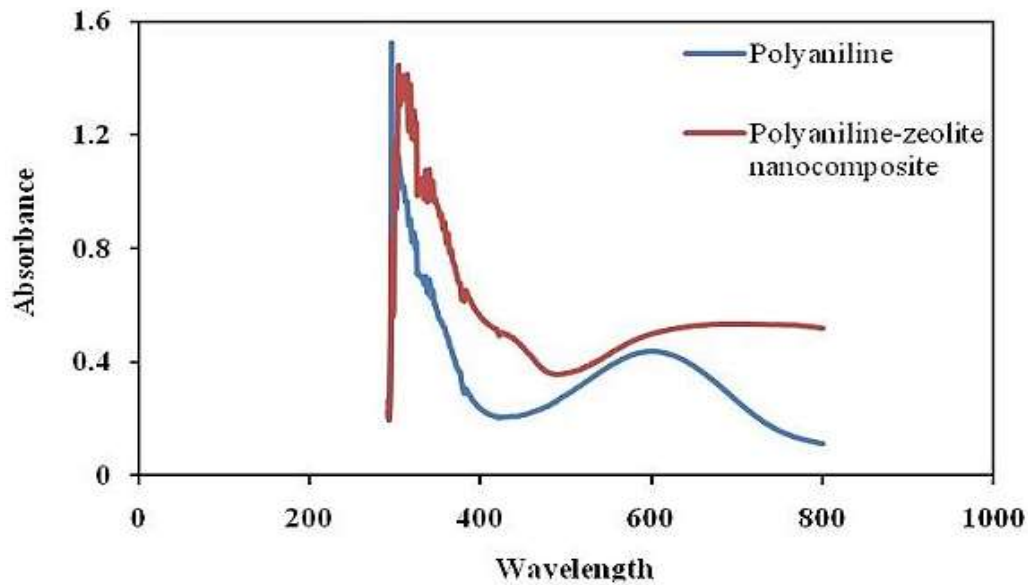


Fig. 4. UV-Vis spectra recorded for polyaniline and polyaniline/zeolite nanocomposite.

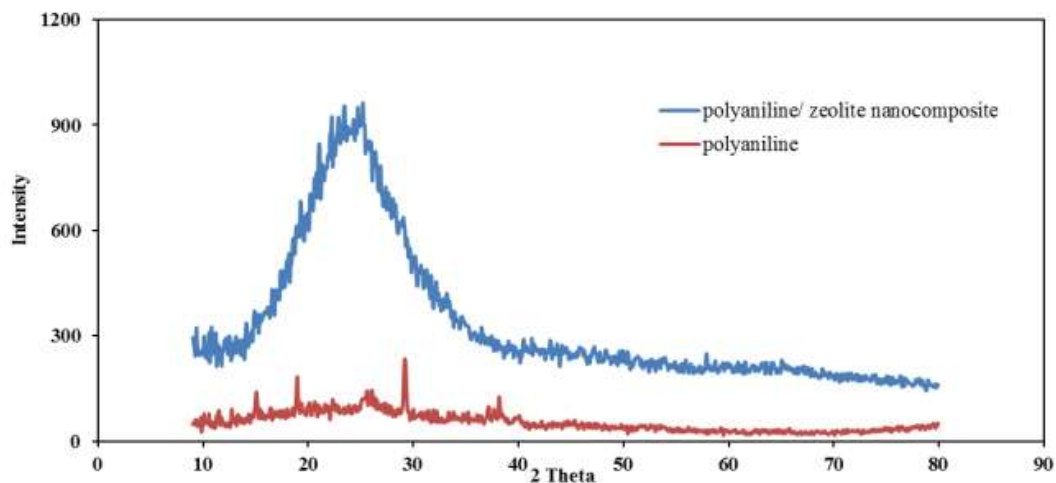


Fig. 5. X-ray diffraction patterns of polyaniline and the polyaniline/zeolite nanocomposite.

polyaniline, reflecting a decreased conjugated chain length of polyaniline in the polyaniline/zeolite nanocomposite.

The X-ray diffraction patterns were recorded for polyaniline/zeolite nanocomposite and polyaniline as presented in Fig. 5. The amount of the XRD pattern peaks can be influenced by crystallinity or by polyaniline chains order in the nanocomposite structure. Fig.5 expressions the XRD pattern of polyaniline that proposes that it has a moderately amorphous structure, but by the encapsulation of polyaniline in the zeolite channel, the arrangement and alignment of polyaniline chain meaningfully upgraded as a result. The amount of these peaks

associated to the nanocomposite was increased [38, 39].

Corrosion protection performance of the coatings

Fig. 6 demonstrates the potentiodynamic polarization curves of the polyaniline/zeolite nanocomposite coating on 304 SS in 0.5 M hydrochloric acid solution. Table 1 presents the several electrochemical parameters obtained from the potentiodynamic polarization curves. The values of E_{corr} , I_{corr} , corrosion rate (CR) and polarization resistance (R_{pol}) are set in Table 1. It was obvious that the current values of the coated sample are lower than that of the bare sample and

corrosion potential of the coated sample is slightly moved to anodic direction. From the measured corrosion current density values, the protection efficiency (PE) was attained from the following equation[2]:

$$PE\% = \frac{I_{corr} - I_{corr(c)}}{I_{corr}} \times 100 \quad (1)$$

where $I_{corr(c)}$ and I_{corr} are the corrosion current densities in the presence and absence of coating, respectively.

The I_{corr} of the un-coated 304 SS was also found to be higher than that of the coated electrode. So, the low I_{corr} values show a superior difficulty to form passive film when compared to un-coated 304 SS. This comportment can be ascribed to

the lower CR content in the polyaniline/zeolite nanocomposite-coated electrode [40].

Metal is oxidized in the acidic solutions to a higher valence state by dissolving in an anodic reaction (R1). The dissolved species in the solution like O_2 and H^+ are reduced by electrons released from metal in a cathodic reaction (R2, R3) [41].



The redox route also takes place between the coating and solution as another cathodic reaction,

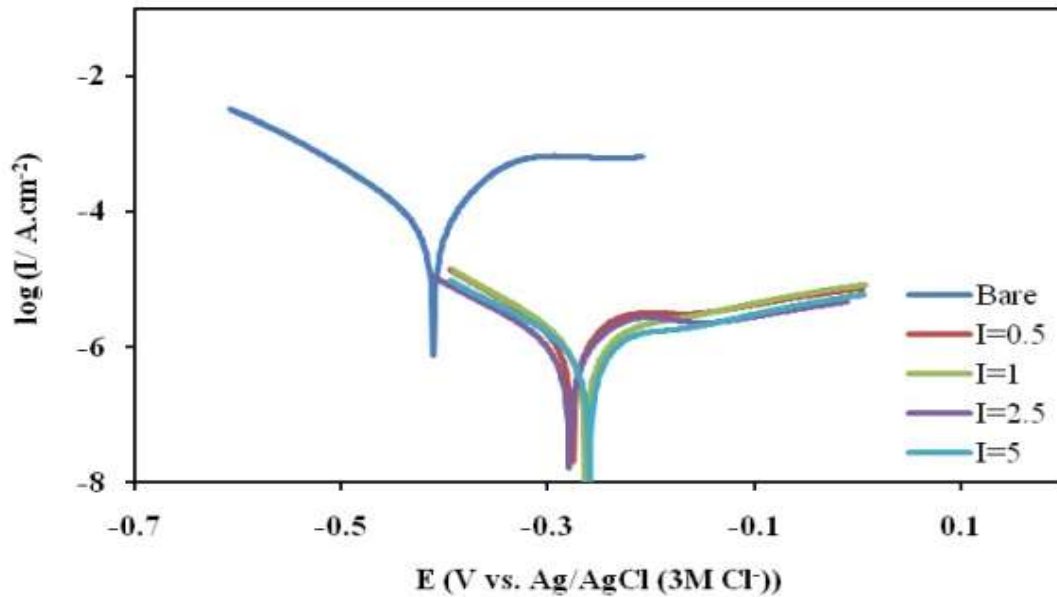


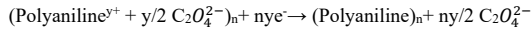
Fig. 6. The polarization behavior of electro-generated polyaniline/zeolite nanocomposite coated on 304 SS at various current densities (mAcm⁻²) in 0.5 M hydrochloric acid medium.

Table 1. Electrochemical factors of electro-generated polyaniline/zeolite nanocomposite coatings on 304 SS in 0.5 M hydrochloric acid medium under the galvanostatic conditions at various applied current densities

Sample	I_{corr} ($\mu A cm^{-2}$)	E_{corr} (V)	R_{pot} ($K\Omega cm^2$)	CR ($mm year^{-1}$)	P^*	PE%
Bare	68.60	-0.411	0.274	0.797	-	-
0.5 mAcm ⁻²	6.57	-0.276	15.416	0.076	0.0009	90.41
1.0 mAcm ⁻²	5.86	-0.264	20.842	0.068	0.0005	90.45
2.5 mAcm ⁻²	1.96	-0.279	21.873	0.022	0.0007	97.13
5.0 mAcm ⁻²	5.86	-0.259	25.877	0.068	0.0004	91.44

b_s : 0.106 Vdec⁻¹

when the polymer-coated electrode is immersed in a corrosive solution. As a outcome of this reaction (R4), the oxalate ions in the polymer structure are removed.



As it can be realized in Table 1, corrosion current densities decrease from 68.60 $\mu\text{A cm}^{-2}$ for un-coated 304 SS to 1.96 $\mu\text{A cm}^{-2}$ for polyaniline/zeolite nanocomposite-coated 304 SS under best settings (2.5 mA cm^{-2}). Also, CR of 304 SS is considerable reduced as a result of the decrease in i_{corr} . The corrosion rate of the coated 304 SS is found to be 0.022 mm year^{-1} , which is nearby 36 times lower than that detected for bare 304 SS.

The polarization resistance (R_{pol}) is a significant factor, that capability of coating in avoidance of electron exchange in a corrosive environment. As it can be gotten in Table 1, R_{pol} increases from 0.274 $\text{k}\Omega \text{cm}^2$ for un-coated 304 SS to 211.873 $\text{k}\Omega \text{cm}^2$ for coated 304 SS under best condition. This displays that the polyaniline/zeolite nanocomposite coating has high polarization resistance. The PE% calculated from potentiodynamic polarization curves data is found to be 97.13% for 2.5 mA cm^{-2} , and PE% a little decreased for current density higher than 2.5 mA cm^{-2} (91.44% for 5 mA cm^{-2}).

Another one of the main parameters, which powerfully governs the anticorrosive performance of the coatings, is coating porosity. Hence, measurement of the coating porosity is important to approximation the whole corrosion protection of the coated substrate. In this research, the porosity of polyaniline/zeolite nanocomposite coated on 304 SS substrates was determined from polarization resistance measurements. The

porosity of polymer coating was calculated using the relation [39]:

$$P = (R_{\text{pol(uc)}} / R_{\text{pol(c)}}) \times 10^{-(\Delta E / b_a)} \quad (2)$$

where P is the total porosity, $R_{\text{pol(c)}}$ is the polarization resistance of coated 304 SS, $R_{\text{pol(uc)}}$ is the polarization resistance of the bare 304 SS, ΔE_{corr} is the difference between potentials of corrosion and b_a ($b_a = 0.106 \text{ V dec}^{-1}$) is the anodic Tafel slope for bare 304 SS substrate. The porosity in polyaniline/zeolite nanocomposite coating obtained at 2.5 mA cm^{-2} was found to be 0.0007. As it can be understood, the porosity was decreased in the existence of zeolite.

So, it can be concluded from the attained results, that the polyaniline/zeolite nanocomposite coating have low porosity in higher current densities, cause decreasing of the corrosion current and also is increasing of PE%.

It appears that the electrode surface is slowly covered as the applied current density is increased by preliminary films of the coating and it continues while the surface of the electrode is completely covered. Then, the depth of the coating increased as the applied current density is more increased and consequently the effectiveness of the coating decreased due to the formation of the defects and cracks that are formed in the thickening period. So, it can be concluded that the polyaniline/zeolite nanocomposite coated on 304 SS have high porosity in the much higher applied currents densities, which causes increases the corrosion current and also, the PE% is slightly reduced. Agreeing to the results, the best current density for the electro-generation of the polyaniline/

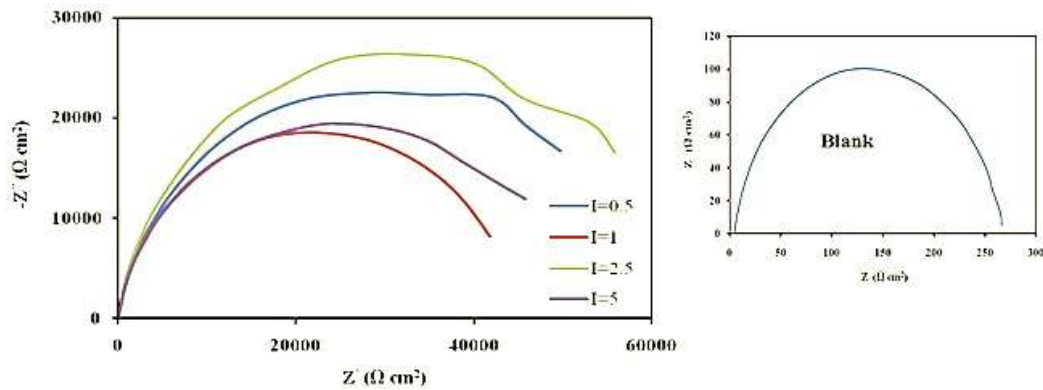


Fig. 7. Nyquist impedance plots for uncoated 304 SS and polyaniline/zeolite nanocomposite coated 304 SS generated under galvanostatic conditions at various current densities (mAcm^{-2}).

zeolite nanocomposite coating on 304 SS with the greatest of corrosion protection performance is 2.5 mA cm⁻².

EIS measurements

To explore the anticorrosive properties of the attained coatings, electrochemical impedance spectroscopy was employed, due to its non-disturbing and informative properties. The typical Nyquist impedance plots of the polyaniline/zeolite nanocomposite-coated 304 SS produced under galvanostatic settings at the various applied current densities are presented in Fig. 7. These impedance plots were modeled by the equivalent circuit showed in Fig. 8. The equivalent circuit contains the electrolyte resistance (R_s), coating capacitance (CPE_c), the coating pore resistance (R_p), charge transfer resistance (R_{ct}) and double layer capacitance (C_{dl}). Instead of capacitance, a constant phase element (CPE) was used. The constant phase element represents the nonconformity from the true capacitance behavior [39].

For the description of a frequency independent phase shift between an applied alternating potential and its current response, a constant phase element (CPE) is used instead of capacitance (C). The CPE is defined by the mathematical expression [42, 43].

$$Z_{CPE} = 1 / Q_0(jw)^n \tag{3}$$

where Z_{CPE} , impedance of CPE; Q_0 , a proportional factor; w , Angular frequency; j , $(-1)^{1/2}$; and n , the exponential term, which has numerous different explanations, it can be related with the roughness of electrode surface [44], a distribution of reaction rates [45], non-uniform current distribution [46], etc. The charge transfer resistance values of un-coated, polyaniline/zeolite nanocomposite-coated 304 SS in 0.5 M hydrochloric acid are 0.2 kΩ cm² and 64.6 kΩ cm² respectively under best condition.

The values of the impedance parameters of the best fit to the experimental impedance plots for un-coated 304 SS and polyaniline/zeolite nanocomposite-coated 304 SS with the equivalent circuits are set in Table 2. The percentage of

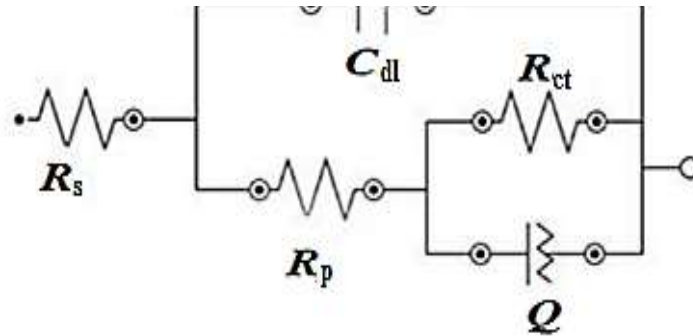


Fig. 8. Equivalent circuit model.

Table 2. Impedance values of the electro-generated polyaniline/zeolite nanocomposite coatings extracted from the fit to the equivalent circuit for the impedance spectra recorded in 0.5 M hydrochloric acid medium.

Sample	R_s (Ω cm ²)	R_{ct} (KΩ cm ²)	C_{dl} (μF cm ²)	R_p (Ω cm ²)	n	Q y^*	d^{**}	PE%
Bare	4.4	0.2	84.7	1.2	0.75	30.5	-	-
0.5 mAcm ⁻²	4.4	58.3	19.3	13.2	0.82	45.3	1.92	99.61
1.0 mAcm ⁻²	5.3	45.4	18.5	11.8	0.83	43.4	2.00	99.49
2.5 mAcm ⁻²	4.3	64.6	18.6	20.7	0.82	38.2	1.99	99.64
5.0 mAcm ⁻²	4.6	49.5	16.46	13.6	0.81	49.1	2.25	99.54

* $Y(\Omega^{-1} \text{cm}^{-2} \text{s}^n)$

** ($\epsilon_0 = 8.85 \times 10^{-12} \text{ F cm}^{-1}$, $\epsilon = 4.2$, $A = 1 \text{ cm}^2$)

protection efficiency (PE%) was calculated using the following equation [47]:

$$PE\% = \frac{R_{ct(c)} - R_{ct}}{R_{ct(c)}} \times 100 \quad (4)$$

where $R_{ct(c)}$ and R_{ct} are the charge transfer resistance in existence and lack of coating, respectively.

The lower values of C_{dl} for the coated-304 SS provide more support for the protection of 304 SS by the polyaniline/zeolite nanocomposite coating. Therefore, the higher value of R_{ct} and lower value of C_{dl} show the outstanding corrosion performance of the polyaniline/zeolite nanocomposite coating. The PE% and R_{ct} calculated from EIS data is found that the values increase with increasing the applied current density up to 2.5 mA cm^{-2} , which is in agreement with the potentiodynamic polarization outcomes.

Computing of coating thickness which is a significant feature for industrial applications is one of the important factors for synthesis of the polymer coatings on the metal surface. EIS data

can be used for measurement of the thickness of the coatings. The thickness of polyaniline/zeolite nanocomposite coating on the surface of 304 SS by using of C_{dl} value can be realized according to the following equation [48]:

$$C_{dl} = \frac{\epsilon_0 \epsilon A}{d} \quad (5)$$

where ϵ is the dielectric constant of the environment, ϵ_0 is the vacuum permittivity; A is the electrode area, and d is the thickness of the protective layer. As can be seen in Table 2, thickness increased and coating capacitance reduced with increasing of applied current density up to 2.5 mA cm^{-2} . According to Table 2, it can be determined that the protection efficiency increased when coating thickness increased. On the other hand, these results show that the barrier properties of the coating on the 304 SS surface increased.

SEM characterization

Fig. 9 displays the typical SEM pictures of abraded 304 SS (image a), prepared 304 SS after corrosion (image b),

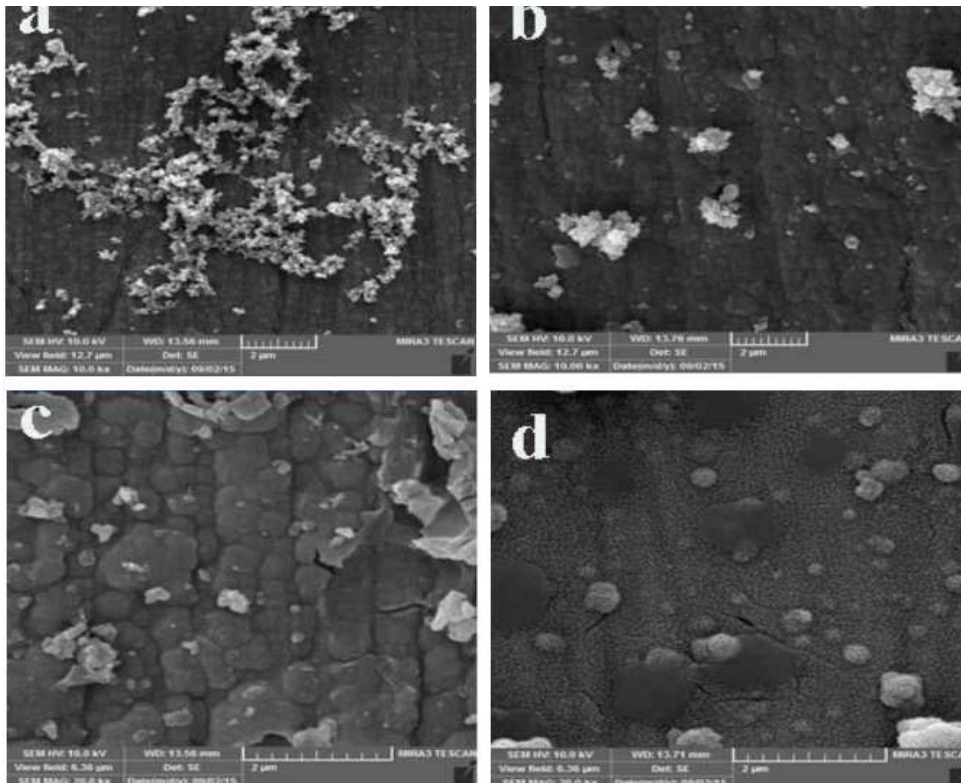


Fig. 9. SEM micrographs of abraded 304 SS electrode (image a), 304 SS electrode after corrosion (image b), polyaniline/zeolite nanocomposite-coated 304 SS electrode (c) and polyaniline/zeolite nanocomposite-coated 304 SS electrode after corrosion (d).

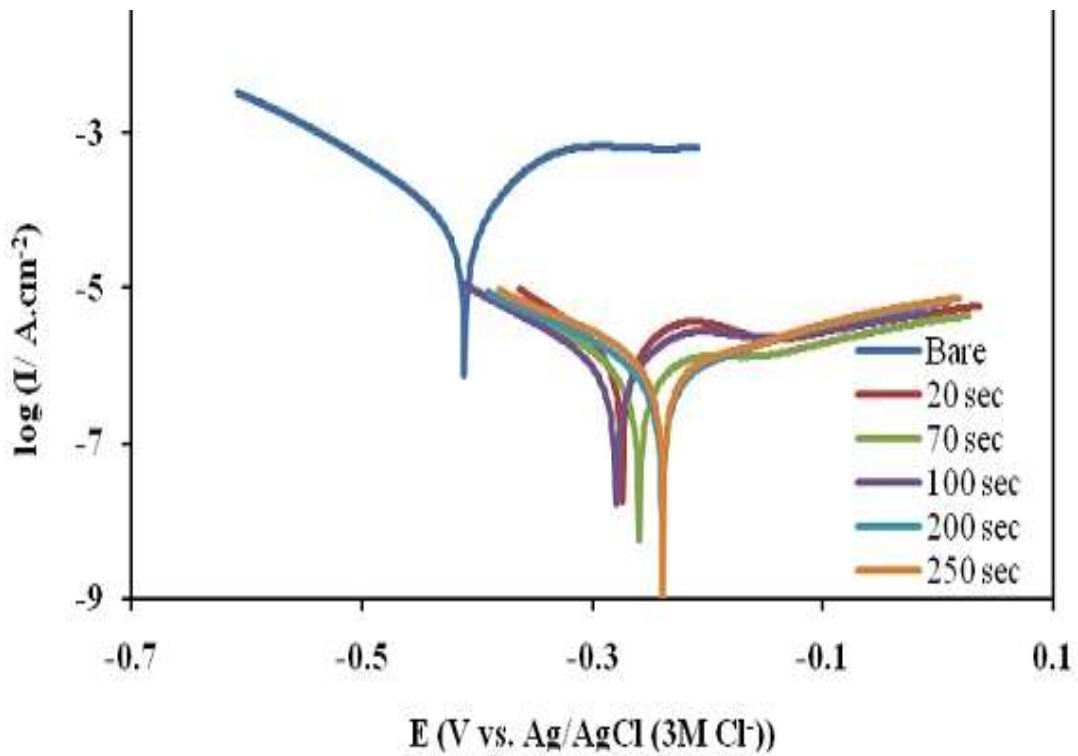


Fig. 10. The polarization behavior of electro-generated polyaniline/zeolite nanocomposite coated on 304 SS at various times (s) in 0.5 M hydrochloric acid medium.

Table 3. Electrochemical parameters of the electro-generated polyaniline/zeolite nanocomposite coating on 304 SS in 0.5 M hydrochloric acid medium under the galvanostatic conditions for 2.5 mAcm⁻² at different deposition times.

Sample	I_{corr} ($\mu\text{A cm}^{-2}$)	E_{corr} (V vs. Ag/AgCl V)	R_{pol} ($\text{K}\Omega \text{cm}^2$)	CR (mm year^{-1})	PE%
Bare	68.60	-0.411	0.274	0.797	-
20 s	9.02	-0.273	12.664	0.105	86.83
70 s	5.37	-0.259	29.294	0.062	92.16
100 s	1.96	-0.279	21.873	0.023	97.13
200 s	4.80	-0.239	31.649	0.056	92.99
250 s	5.05	-0.238	23.651	0.059	92.63

(image b), 304 SS coated with polyaniline/zeolite nanocomposite grown by an applied current density of 2.5 mA cm⁻² for 100 s (image c) and the polyaniline/zeolite nanocomposite coated 304 SS after corrosion (image d). A judgment of pictures (a) and (b) displays that many large inequalities

and pits were formed after corrosion, which reveals severe damage on surface due to metal dissolution. Image d displays that the polyaniline/zeolite nanocomposite coating was electro-generated on the surface and protected it from the corrosion.

Effect of deposition time on the corrosion protection performance

Fig. 10 displays the potentiodynamic polarization curves of the nanocomposite coatings on 304 SS in 0.5 M hydrochloric acid solution at several deposition times for the best of applied current density (2.5 mA cm^{-2}) and the values of the related factors are summarized in Table 3. Study of these data displays that the corrosion current and CR values decreased when the deposition time was increased up to 100 s, but I_{corr} and CR values increased when the deposition time was more than 100 s. In the other word, the most operative protection against corrosion in an aqueous neutral corrosive medium was accomplished when the used deposition time was 100 s.

CONCLUSIONS

The polyaniline/zeolite nanocomposite coatings were well direct electro-generated on 304 SS substrates from aqueous solutions containing oxalic acid and aniline monomers with dispersed zeolite nanoparticles. Adherent, uniform and compact coatings can be attained under galvanostatic condition. Four various current densities of 0.5, 1, 2.5 and 5 mA cm^{-2} were applied for the creation of polyaniline/zeolite nanocomposite coatings on 304 SS. The results presented that applying the current density of 2.5 mA cm^{-2} with a time duration of 100 s for the electro-generation is the best setting for the preparation of strongly adherent and more compact polyaniline/zeolite nanocomposite coatings on 304 SS. The coatings were characterized by FT-IR, UV-Vis and XRD and the corrosion protection performance of the electro-generated coatings were assessed using Tafel polarization and electrochemical impedance spectroscopy in 0.5 M hydrochloric acid solution. The EIS outcomes are in good agreement with the Tafel polarization measurements. This research discloses the polyaniline/zeolite nanocomposite coating has good corrosion protection properties and can be considered as a possible coating material to protect 304 SS against corrosion in solution 0.5 M hydrochloric acid solution. It is believed that the coating assistances to stabilize the passive film onto the substrate thus ending the 304 SS corrosion.

The existence of zeolite particles dispersed in polyaniline matrix increase the tortuosity of the diffusion pathway of corrosive agents such as O_2 , H^+ , OH^- and Cl^- ions.

ACKNOWLEDGMENT

The authors are grateful to University of Kashan for supporting this work by Grant No (573591-5).

CONFLICT OF INTEREST

The authors declare that there are no conflicts of interest regarding the publication of this manuscript.

REFERENCES

1. Shabani-Nooshabadi M, Ghandchi MS. Santolina chamaecyparissus extract as a natural source inhibitor for 304 stainless steel corrosion in 3.5% NaCl. *J. Ind. Eng. Chem.* 2015;31:231-237.
2. Shabani-Nooshabadi M, Ghoreishi SM, Behpour M. Direct electrosynthesis of polyaniline-montmorillonite nanocomposite coatings on aluminum alloy 3004 and their corrosion protection performance. *Corros Sci.* 2011;53(9):3035-3042.
3. Gopi D, Govindaraju KM, Kavitha L, Basha KA. Synthesis, characterization and corrosion protection properties of poly(N-vinyl carbazole-co-glycidyl methacrylate) coatings on low nickel stainless steel. *Prog Org Coat.* 2011;71(1):11-18.
4. Ganash AA, Al-Nowaiser FM, Al-Thabaiti SA, Hermas AA. Protection of stainless steel by the electrodeposition of polyaniline/poly(o-phenylenediamine) composite layers. *J Solid State Electrochem.* 2012;17(3):849-860.
5. Sathiyarayanan S, Karpakam V, Kamaraj K, Muthukrishnan S, Venkatachari G. Sulphonate doped polyaniline containing coatings for corrosion protection of iron. *Surf Coat Technol.* 2010;204(9-10):1426-1431.
6. Ali Fathima Sabirneeza A, Subhashini S. A novel water-soluble, conducting polymer composite for mild steel acid corrosion inhibition. *J Appl Polym Sci.* 2012;127(4):3084-3092.
7. Negm NA, Ghuiba FM, Tawfik SM. Novel isoxazolium cationic Schiff base compounds as corrosion inhibitors for carbon steel in hydrochloric acid. *Corros Sci.* 2011;53(11):3566-3575.
8. Ganash AA, Al-Nowaiser FM, Al-Thabaiti SA, Hermas AA. Comparison study for passivation of stainless steel by coating with polyaniline from two different acids. *Prog Org Coat.* 2011;72(3):480-485.
9. Okazaki Y, Gotoh E. Metal release from stainless steel, Co-Cr-Mo-Ni-Fe and Ni-Ti alloys in vascular implants. *Corros Sci.* 2008;50(12):3429-3438.
10. Patil S, Mahajan JR, More MA, Patil PP, Gosavi SW, Gangal SA. Electrochemical polymerization of poly(o-anisidine) thin films: effect of synthesis temperature studied by cyclic voltammetry. *Polym Int.* 1998;46(2):99-105.
11. Ates M, Sarac AS. Conducting polymer coated carbon surfaces and biosensor applications. *Prog Org Coat.* 2009;66(4):337-358.
12. Olad A, Rashidzadeh A. Preparation and anticorrosive properties of PANI/Na-MMT and PANI/O-MMT nanocomposites. *Prog Org Coat.* 2008;62(3):293-298.
13. Sathiyarayanan S, Azim SS, Venkatachari G. Corrosion protection of magnesium ZM 21 alloy with polyaniline-TiO₂ composite containing coatings. *Prog Org Coat.* 2007;59(4):291-296.
14. Hermas AA, Salam MA, Al-Juaid SS, Qusti AH, Abdelaal MY. Electrosynthesis and protection role of polyaniline-polvinylalcohol composite on stainless steel. *Prog Org Coat.* 2014;77(2):403-411.

15. Peng C-W, Chang K-C, Weng C-J, Lai M-C, Hsu C-H, Hsu S-C, et al. Nano-casting technique to prepare polyaniline surface with biomimetic superhydrophobic structures for anticorrosion application. *Electrochim Acta*. 2013;95:192-199.
16. Kalendová A, Veselý D, Stejskal J, Trchová M. Anticorrosion properties of inorganic pigments surface-modified with a polyaniline phosphate layer. *Prog Org Coat*. 2008;63(2):209-221.
17. Abaci S, Nessark B. Characterization and corrosion protection properties of composite material (PANI+TiO₂) coatings on A304 stainless steel. *Journal of Coat. Tech. Res*. 2014;12(1):107-120.
18. Yeh J-M, Chang K-C. Polymer/layered silicate nanocomposite anticorrosive coatings. *J. Ind. Eng. Chem*. 2008;14(3):275-291.
19. Gao H, Xiao F, Ching CB, Duan H. One-Step Electrochemical Synthesis of PtNi Nanoparticle-Graphene Nanocomposites for Nonenzymatic Amperometric Glucose Detection. *ACS. Appl. Mat. Inter*. 2011;3(8):3049-3057.
20. Shi J-J, Zhu J-J. Sonoelectrochemical fabrication of Pd-graphene nanocomposite and its application in the determination of chlorophenols. *Electrochim Acta*. 2011;56(17):6008-6013.
21. Wang S, Tan Z, Li Y, Sun L, Zhang T. Synthesis, characterization and thermal analysis of polyaniline/ZrO₂ composites. *Thermochim Acta*. 2006;441(2):191-194.
22. Gurunathan K, Trivedi DC. Studies on polyaniline and colloidal TiO₂ composites. *Mater Lett*. 2000;45(5):262-268.
23. Qiu G, Wang Q, Nie M. Polyaniline/FE3O4 magnetic nanocomposite prepared by ultrasonic irradiation. *J Appl Polym Sci*. 2006;102(3):2107-2111.
24. Fei Fang F, Hye Kim J, Jin Choi H, Seo Y. Organic/inorganic hybrid of polyaniline/BaTiO₃ composites and their electrorheological and dielectric characteristics. *J Appl Polym Sci*. 2007;105(4):1853-1860.
25. Nghia ND, Tung NT. Study on synthesis and anticorrosion properties of polymer nanocomposites based on super paramagnetic Fe₂O₃.NiO nanoparticle and polyaniline. *Synth Met*. 2009;159(9-10):831-834.
26. Ruiz-Hitzky E, Aranda P. Confinement of conducting polymers into inorganic solids, *Anales de química*, Springer, 1997, pp. 197-212.
27. Cardin DJ. Encapsulated Conducting Polymers. *Adv Mater*. 2002;14(8):553.
28. Dalas E, Vitoratos E, Sakkopoulos S, Malkaj P. Polyaniline/zeolite as the cathode in a novel gel electrolyte primary dry cell. *J Power Sources*. 2004;128(2):319-325.
29. Vitoratos E, Sakkopoulos S, Dalas E, Malkaj P, Anestis C. D.C. conductivity and thermal aging of conducting zeolite/polyaniline and zeolite/polypyrrole blends. *Curr. Appl. Phys*. 2007;7(5):578-581.
30. Iroh JO, Zhu Y, Shah K, Levine K, Rajagopalan R, Uyar T, et al. Electrochemical synthesis: a novel technique for processing multi-functional coatings. *Prog Org Coat*. 2003;47(3-4):365-375.
31. Shirakawa H, Louis EJ, MacDiarmid AG, Chiang CK, Heeger AJ. Synthesis of electrically conducting organic polymers: halogen derivatives of polyacetylene, (CH)_x. *J Chem Soc, Chem Commun*. 1977(16):578.
32. Sambyal P, Ruhi G, Dhawan R, Dhawan SK. Designing of smart coatings of conducting polymer poly(aniline-co-phenetidine)/SiO₂ composites for corrosion protection in marine environment. *Surf Coat Technol*. 2016;303:362-371.
33. Yeh J-M, Chen C-L, Chen Y-C, Ma C-Y, Lee K-R, Wei Y, et al. Enhancement of corrosion protection effect of poly(o-ethoxyaniline) via the formation of poly(o-ethoxyaniline)-clay nanocomposite materials. *Polymer*. 2002;43(9):2729-2736.
34. Kamaraj K, Sathiyarayanan S, Venkatachari G. Electropolymerised polyaniline films on AA 7075 alloy and its corrosion protection performance. *Prog Org Coat*. 2009;64(1):67-73.
35. Kamaraj K, Karpakam V, Sathiyarayanan S, Venkatachari G. Electrosynthesis of Polyaniline Film on AA 7075 Alloy and Its Corrosion Protection Ability. *J Electrochem Soc*. 2010;157(3):C102.
36. S.M.Ghoreishi, Shabani-Nooshabadi M, Behpour M, Jafari Y. Electrochemical synthesis of poly(o-anisidine) and its corrosion studies as a coating on aluminum alloy 3105. *Prog Org Coat*. 2012;74(3):502-510.
37. Pron A, Genoud F, Menardo C, Nechtschein M. The effect of the oxidation conditions on the chemical polymerization of polyaniline. *Synth Met*. 1988;24(3):193-201.
38. Shyaa AA, Hasan OA, Abbas AM. Synthesis and characterization of polyaniline/zeolite nanocomposite for the removal of chromium(VI) from aqueous solution. *J. Sau. Chem. Soc*. 2015;19(1):101-107.
39. Shabani-Nooshabadi M, Karimian-Taheri F. Electrosynthesis of a polyaniline/zeolite nanocomposite coating on copper in a three-step process and the effect of current density on its corrosion protection performance. *RSC Advances*. 2015;5(117):96601-96610.
40. Rovere CAD, Alano JH, Otubo J, Kuri SE. Corrosion behavior of shape memory stainless steel in acid media. *J Alloys Compd*. 2011;509(17):5376-5380.
41. Zeybek B, Aksun E, Üge A. Investigation of corrosion protection performance of poly(N-methylpyrrole)-dodecylsulfate/multi-walled carbon nanotubes composite coatings on the stainless steel. *Mater Chem Phys*. 2015;163:11-23.
42. Ashassi-Sorkhabi H, Seifzadeh D, Hosseini MG. EN, EIS and polarization studies to evaluate the inhibition effect of 3H-phenothiazin-3-one, 7-dimethylamin on mild steel corrosion in 1M HCl solution. *Corros Sci*. 2008;50(12):3363-3370.
43. Roeper DF, Chidambaram D, Clayton CR, Halada GP. Development of an environmentally friendly protective coating for the depleted uranium-0.75wt.% titanium alloy. *Electrochim Acta*. 2008;53(5):2130-2134.
44. Mulder WH, Sluyters JH, Pajkossy T, Nyikos L. Tafel current at fractal electrodes. *J. Electroanal. Chem. Inter. Electrochem*. 1990;285(1-2):103-115.
45. Kim C-H, Pyun S-I, Kim J-H. An investigation of the capacitance dispersion on the fractal carbon electrode with edge and basal orientations. *Electrochim Acta*. 2003;48(23):3455-3463.
46. Jorcin J-B, Orazem ME, Pébère N, Tribollet B. CPE analysis by local electrochemical impedance spectroscopy. *Electrochim Acta*. 2006;51(8-9):1473-1479.
47. Tamil Selvi S, Raman V, Rajendran N. Corrosion inhibition of mild steel by benzotriazole derivatives in acidic medium. *J Appl Electrochem*. 2003;33(12):1175-1182.
48. Shabani-Nooshabadi M, Mollahoseiny M, Jafari Y. Electropolymerized coatings of polyaniline on copper by using the galvanostatic method and their corrosion protection performance in HCl medium. *Surf Interface Anal*. 2014;46(7):472-479.